

Asymmetric Dirac cones in monatomic hexagonal lattices.

A. M. Rojas-Cuervo and R. R. Rey-González*

*Departamento de Física, Universidad Nacional de Colombia,
Ciudad Universitaria, C.P. 111321, Bogotá D.C. Colombia.*

(Dated: April 17, 2013)

The study of nanostructures has contributed to the advance of an interdisciplinary science as nanotechnology is. Among those ones, graphene has been distinguished in the last years by its interesting properties and specially, in our own interest, the presence of Dirac cones in electronic dispersion relation. This material is considered the cornerstone in further scientific and technological innovation. In this theoretical paper, crystallographic phase systems similar to graphene, such as silicon hexagonal monolayer (h-Si) or germanium (h-Ge), are analyzed, using the density functional theory (DFT), implemented in the code SIESTA, in the generalized gradient approximation (GGA), into the Perdew-Burke-Ernzerhof functional (PBE) and optimized norm-conserving pseudopotentials. The results found permit us to report the chemical stability of h-Ge. Also, the lattice parameters, electronic dispersion relations and the density of states (DOS) for graphene, h-Si and h-Ge are reported. The existence of Dirac cones is seen in the electronic dispersion relation for each one of the studied hexagonal monolayers. The cones show lateral asymmetry in function of the direction around the K point. In particular, Fermi velocities are calculated for holes and electrons in function of the direction.

I. INTRODUCTION

Currently, the nanotechnology boom as multidisciplinary science is owing to the construction and characterization of a wide variety of materials with low dimensionality as much as organic, inorganic or mixed types¹. Recently one of the most important results has been isolating the graphene through mechanical exfoliation². This monolayer of carbon atoms prepared in hexagonal form accounts for two dimensional structure material which existence should be impossible due to thermodynamic instability showed by L. Landau and R. Peierls' theory^{3,4}.

Graphene has been investigated either in theory or experimentally way^{2,5,6}, finding in its dispersion relation, the absence of an energy gap, with an innovative characteristic such as the linearity of conduction and valence bands around Fermi level that is found in the reciprocal lattice K -point. In these zones known as Dirac cones, electrons and holes behave as quasiparticles without mass and with an effective speed $c^* \approx 10^6$ m/s, independent of its wavevector. In front of this important discovering, we wonder ourselves if other stable materials can exist in two dimensional form and show linearity in its electronic dispersion relation.

Searching for those answers has motivated the development of this work to explore structural and electronic properties of materials which through years have had a huge diversity on technological applications such as: Si (Silicon) and Ge (Germanium), but now in hexagonal monolayer forms (h-Si, h-Ge). In theoretical investigation of low dimensional systems, formalisms of first principles or *ab initio* have been used in its Density Functional Theory (DFT) formulation. In particular, the SIESTA code implementation (*Spanish Initiative for Electronic Simulations with Thousands of Atoms*)⁷ is employed in the academic environment⁸ as in the industrial⁹

or applied investigation¹⁰. This article is organized as follows. In section II some computer details relate with the method are introduced, in section III some relevant physical parameters are reported. In sections IV and V we show the electronic dispersion relations, Density of States (DOS) and the analysis of the Dirac cones for these materials.

II. COMPUTER DETAILS

In the study of electronic and structural properties of h-C, h-Si and h-Ge monolayers, we use SIESTA code, which useful to realize calculations of electronic structure or vibrational properties and geometrical optimization by simulations of molecular dynamic. Besides, It employs efficient algorithms permitting a medium level computer cost, due to the time of linearly scale calculus with the number of system atoms. In the study of our systems, the only initial information provided to the code is the number and the type of atoms that compounds each system with their approximated positions in the hexagonal structure and lattice parameter. In the calculus of interchange and correlation energy is used the gradient generalized approximation (GGA) with the Perdew-Burke-Ernzerhof functional (PBE)¹¹. Valence electrons are described for localized numerical atomic orbitals (NAO) with a double- ζ base polarization (DZP) and core electrons are treated implicitly with norm-conserving pseudopotentials^{12,13} and optimized cut off radii r_c ^{14,15}. The analysis of the chemical stability of the structures is realized through a relaxation process, in which the unit cell atoms are moved slowly, step by step, minimizing the strength among them and with 200 interactions per step. A chemical structure is considered stable for a maximum atomic force tolerance of 40 meV Å⁻¹⁶. In the analyzed systems, stability was found before

2000 steps.

III. LATTICE PARAMETERS

Lattice parameters for different bidimensional hexagonal sheets are found through a relaxation process by dynamic molecular, in which chemical stability is determined of these systems according to values mentioned above. In particular, the data found for bond length a_0 , lattice constant a and maximum atomic force tolerance f_{tol} in the process of relaxation are reported in the table I. As a way of method validation are included the values found for graphene, which are in good agreement with previous theoretical and experimental reports up to 99%^{17–19}.

TABLE I. Bond length a_0 , lattice constant a and maximum atomic force tolerance f_{tol} of hexagonal monolayers, including spin effects (cs) and absence of these (ss).

Monocapa	a_0 (Å)	a (Å)	f_{tol} (eVÅ ⁻¹)
h-C (ss)	1.419	2.458	0.9×10^{-3}
h-C (cs)	1.419	2.458	0.002
h-Si (ss)	2.230	3.860	0.3×10^{-3}
h-Si (cs)	2.230	3.860	0.2×10^{-3}
h-Ge (ss)	2.310	4.001	0.001
h-Ge (cs)	2.310	4.001	0.030

In case of h-Si, the values reported depend on substrate used in their growth. In substrates of $A_g(110)$ the lattice parameter reported is 3.88 Å ²⁰, using $A_g(111)$ the value is $a = 3.3 \text{ Å}$ ²¹ and $a = 3.65 \text{ Å}$ for (0001) – ZrB_2 ²². When these results are compared with ours, we found differences of 0.46%, 14.55% and 5.49%, respectively.

IV. DISPERSION RELATIONS AND DENSITY OF STATES OF STATES

Silicon (Si) and Germanium (Ge) structures in their three-dimensional form are equivalent to the diamond one with indirect energy gaps E_g of 1.12 eV and 0.67 eV to $T = 300 \text{ K}$ ^{23,24}, respectively, showing a semiconductor behavior. For bidimensional materials, *i. e.* hexagonal sheets, after the relaxation process which permits to obtain the lattice parameter, the electronic dispersion relation is calculated, either with spin effects (ss) or including them (cs).

In particular, for graphene, spin effects are evidents to high energies while for values around Fermi levels, significant changes are not observed in the DOS, see Figs. 1 y 2. Nevertheless, including spin effects generates relevant changes in the dispersion relation and specially in the Dirac cones, such as it can be observed in Fig. 3, where there are an enlargement for electronic dispersion relations around K -point without including spin effects (ss), left panel, and including them (cs), right panel. Main

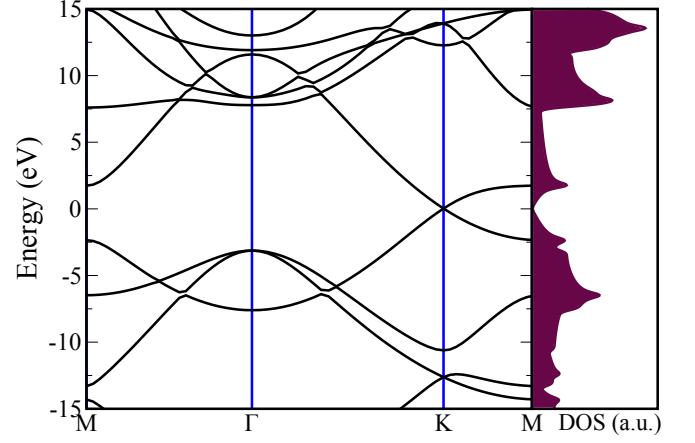


FIG. 1. Electronic dispersion relation and density of states (DOS) for a hexagonal monolayer of graphene without spin effects (ss).

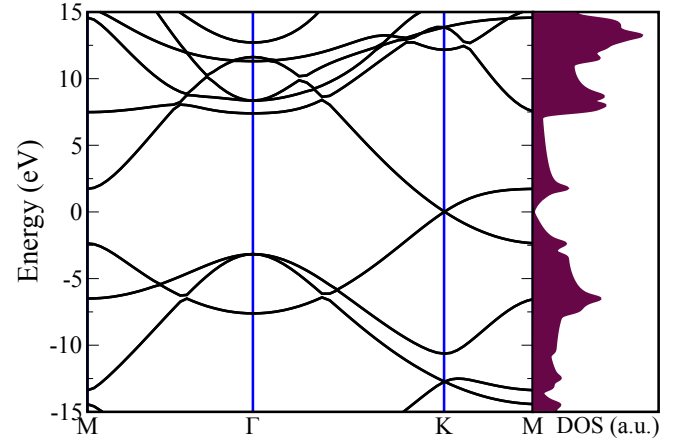


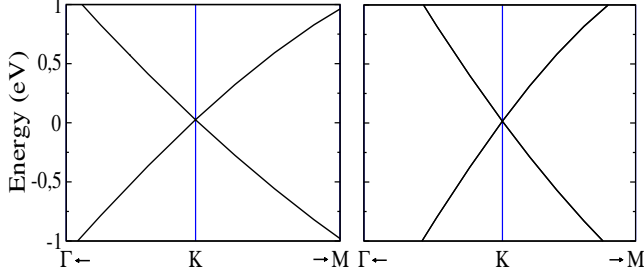
FIG. 2. Electronic dispersion relation and density of states (DOS) for a hexagonal monolayer of graphene with spin effects (cs).

observed changes refer to the Fermi speed both for electrons and holes and an lateral asymmetry of each one of the Dirac cones as function of approaching direction to K point. Previous theoretical results using models type tight binding²⁵, do not show this lateral asymmetry, neither the difference among speed values of the electrons and holes, which has been observed experimentally such as Kai-Chieh Chuang *et al*²⁶ and Jiam Xue *et al*²⁷ report.

In the case of h-Si and h-Ge, a semimetal characteristic is observed, *i. e.*, the non existence of an energy gap between valence and conduction bands, see Figs. 4 and 5. These ones get intersection punctually around K , equivalent to what occurs in graphene. Characteristic that is confirmed in DOS for each case, as it can be seen in the right panel of the corresponding dispersion relations. Previous results report that h-Si is a direct bandgap semiconductor as show the table II. Our results indicate that h-Si and h-Ge are semimetal systems, instead of spin effects are included or not.

TABLE II. Energy gap values in eV.

System	Ref. ²⁸	Ref. ²⁹	Ref. ³⁰	Ref. ³¹	Ref. ³²	Ref. ³³	Ref. ³⁴	Here
h-Si	Semimetal	Semimetal	-	Metal	Metal	0.064(Direct)	Semimetal	Semimetal
h-Ge	Semimetal	Metal	Metal	-	$E_g \neq 0$	-0.444(Semimetal)	Semimetal	Semimetal

FIG. 3. Enlargement for electronic dispersion relation around K -point for graphene, without including spin effects (ss), left panel, and including them (cs), right panel.

Dispersion relation of h-Si and h-Ge show a linear behavior around Fermi level, giving rise to Dirac cones, Figs.6 y 7, equivalent to results for graphene *i. e.*, in these materials quantum electrodynamics experiments (QED) could be developed, also.

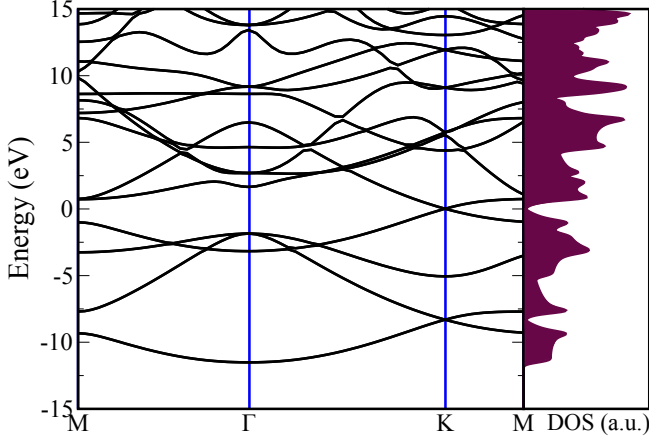


FIG. 4. Electronic dispersion relation and density of states (DOS) for h-Si with spin effects (cs).

In Figs. 6 and 7 there are enlargements of electronic dispersion relations around K -point for h-Si and h-Ge where is possible to visualize lateral asymmetry for the Dirac cones and different velocities between electrons and holes, without considering spin, left panel, and including its effect, right panel. These lateral asymmetries and differences are similar to the ones discussed for graphene.

A quantitative analysis of dispersion relation at Dirac cones permits to determinate Fermi speeds for electrons and holes, in each of the studied materials. For this purpose, a linear regression is done in $\Gamma \rightarrow K$ and of $M \rightarrow K$ directions. Results are showed in the table III, where lateral asymmetry for Fermi speed is evidenced

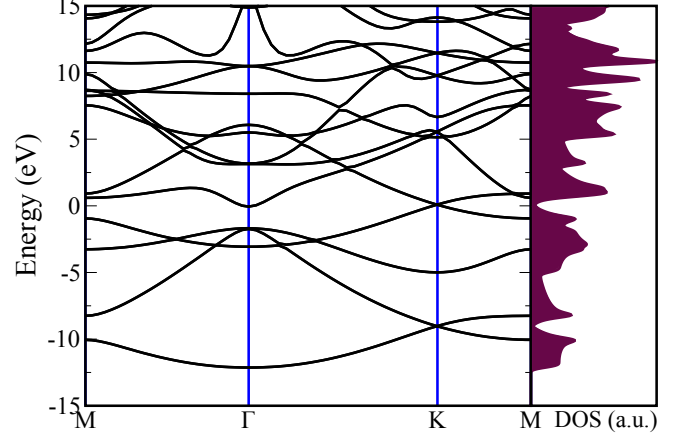
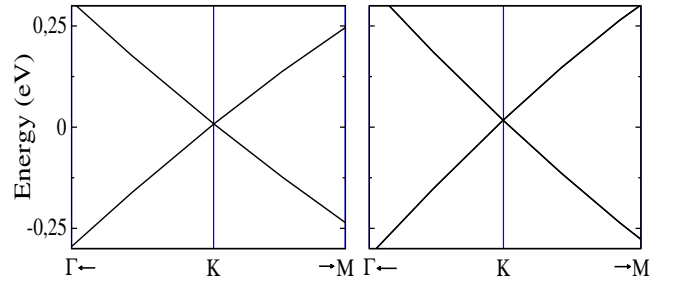


FIG. 5. Electronic dispersion relation and density of states (DOS) for a Ge hexagonal monolayer with spin effects (cs).

either for electrons or holes. The relative variation of Fermi speed to the electrons, in function of the wavevector $\vec{k} = k_x\hat{i} + k_y\hat{j}$, between the two analyzed directions is 61,4% for h-Si(cs), of 45.9% for h-Ge(cs) and of 36.6% for graphene (cs). Equivalent differences are found for Dirac cones holes. In h-Si(cs) there is a relative variation of 57.5%, in h-Ge(cs) of 48.5% and of 28.7% for graphene (cs).

FIG. 6. Enlargement for electronic dispersion relation around K -point for h-Si, without including spin effects (ss), left panel, and including them (cs), right panel.

Experimental results report Fermi speeds of electrons in graphene of $1.093 \times 10^6 \text{ m/s}^{26}$, $0.79 \times 10^6 \text{ m/s}^{35}$, $1.10 \times 10^6 \text{ m/s}^{36}$, $1.16 \pm 0.01 \times 10^6 \text{ m/s}$ and for holes of $0.94 \pm 0.02 \times 10^6 \text{ m/s}^{27}$. In h-Si experimental results give a value of $1.3 \times 10^6 \text{ m/s}$ for Fermi speed of electrons and holes³⁷. For h-Ge, so far we know, there are no experimental speed reports.

The relative variation of Fermi speed for electrons and holes, in function of the k -space directions, indicate that

TABLE III. Fermi speeds V_f ($\times 10^6 m/s$) for electrons and holes, in graphene, h-Si and h-Ge. Without spin effects (ss) and including them (cs).

		electrons		holes	
		$v_f(\Gamma \rightarrow K)$	$v_f(K \rightarrow M)$	$v_f(\Gamma \rightarrow K)$	$v_f(K \rightarrow M)$
h-C	ss	1.406	0.998	1.409	0.996
	cs	1.365	0.999	1.385	1.076
h-Si	ss	1.478	1.078	1.550	1.062
	cs	1.509	0.935	1.533	0.973
h-Ge	ss	1.644	1.047	1.569	0.981
	cs	1.746	1.197	1.639	1.104

this is not constant, presenting a spacial dependence or anisotropy. In recent experimental reports^{36,38–40} is measured a renormalization of Fermi speed. This feature is not unique of the graphene, being shared by other monoatomic bidimensional hexagonal lattices such as: h-Si and el h-Ge. Theoretical results, not show here, indicate that diatomic hexagonal monolayers have not present this behavior⁴¹.

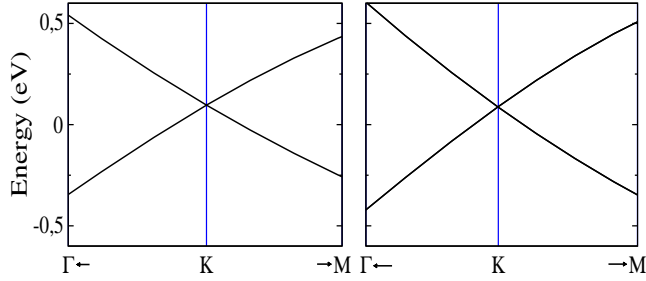


FIG. 7. Enlargement for electronic dispersion relation around K -point for h-Ge, without including spin effects (ss), left panel, and including them (cs), right panel.

V. CONCLUSIONS

Lateral asymmetry or spatial dependence of Fermi speed for electrons and holes is reflected in asymmetric Dirac cones, as it can be observed in Figs. 8(a) and 8(b). These cones are obtained from DFT calculus using SIESTA implementation. In particular, we use the dispersion relations from some M , Γ and K -points neighbors to K -point at $(\frac{2}{3}, \frac{2\sqrt{3}}{3})$. Fig 8(a) corresponds to h-Si case while Fig.8(b) for h-Ge. In both cases, it is possible to identify two type of asymmetries. i) A lateral asymmetry that deform the Dirac cone far away from a circular shaped. ii) An an asymmetry electron-hole *i. e.*, different Dirac velocities for valence and conduction bands. Hole Dirac cones show less height compared with the electrons ones, being this difference stronger for h-Ge, indicating that behavior type no massive Dirac Fermions for holes is

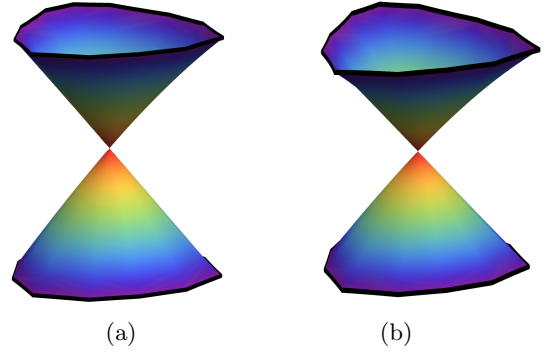


FIG. 8. Dirac cones in 3D for holes and electrons in h-Si and h-Ge with spin effects (cs). Color online

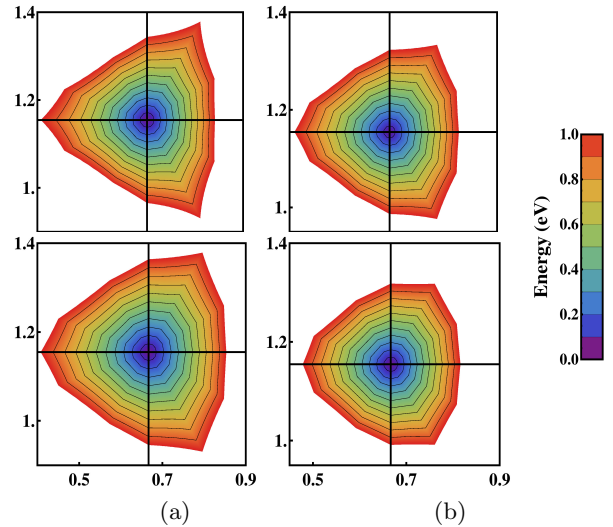


FIG. 9. Contours levels for the energy of for h-Si and h-Ge with spin effects (cs). Color online

lost rapidly at the same time that the wavevector get distant from K point. This characteristic can be important

in experiments that involve magnetic fields or phonon assisted transitions. In Figs. 9 there are energy level curves or equi-energy contours at Dirac cones for holes, upper panels, and for electrons, lower panels, in h-Si Fig.9a and h-Ge Fig. 9b. The intensity of colors represents the energy magnitude in relation with the Fermi level. In each case 10 contour lines are shown. Clearly, there are not circular profiles respect to point K . Lateral asymmetry is represented for the wavevector magnitude variations, or the distance from K -point to each one level curves. In particular, Dirac cones radial asymmetry for holes is bigger in comparison with Electron Dirac cones. From

Dirac equation for no massive Fermions given by:²⁵

$$E_{\pm}(\vec{k}) \approx \pm v_F \|\vec{k}\|, \quad (1)$$

wavevector variations over each one of these constant energy lines implies Fermi speed must do it too, revealing a spatial asymmetry of this speed.

ACKNOWLEDGMENTS

Authors would like to thank the financial support from Division de Investigación Sede Bogotá, Universidad Nacional de Colombia, (DIB).

-
- * rrreyg@unal.edu.co.
- ¹ C. Poole and F. Owens, *Introducción a la Nanotecnología* (Reverté, 2003).
 - ² K. S. Novoselov, A. K. Geim, S. V. Morozov, D. Jiang, Y. Zhang, S. V. Dubonos, I. V. Grigorieva, and A. A. Firsov, *Science* **306**, 666 (2004).
 - ³ R. Peierls, *Ann. I. Poincaré* **5**, 177 (1935).
 - ⁴ L. Landau, *Phys. Z. Sowjetunion* **11**, 26 (1937).
 - ⁵ K. S. Novoselov, A. K. Geim, S. V. Morozov, D. Jiang, M. I. Katsnelson, I. V. Grigorieva, S. V. Dubonos, and A. A. Firsov, *Nature* **438**, 197 (2005).
 - ⁶ A. K. Geim and K. S. Novoselov, *Nat. Mater.* **6**, 183 (2007).
 - ⁷ J. M. Soler, E. Artancho, J. D. Gale, A. García, J. Junquera, P. Ordejón, and D. Sánchez, *J. Phys. Condens. Matter* **14**, 2745 (2002).
 - ⁸ S. Reich, C. Thomsen, and P. Ordejón, *Phys. Rev. B* **65**, 155411 (2002).
 - ⁹ In the industry field, Motorola in 1999 used code SIESTA in the strontium titanium growth on silicon.
 - ¹⁰ The code SIESTA is used in research centers as: NERSC (National Energy Research Scientific Computing Center), CESGA (Centro de Supercomputación de Galicia), NNIN (National Nanotechnology Infrastructure Network) among others.
 - ¹¹ J. P. Perdew, K. Burke, and M. Ernzerhof, *Phys. Rev. Lett.* **77**, 3865 (1996).
 - ¹² N. Troullier and J. L. Martins, *Phys. Rev. B* **43**, 1993 (1991).
 - ¹³ A. García, *ATOM user manual* (ICMAB-CSIC, Bilbao, 2008).
 - ¹⁴ C. A. Pabón-Espejo, *Cálculo de la energía de enlace de las bases nitrogenadas Guanina-Citosina y Adenina-Timina.*, Master's thesis, Universidad Nacional de Colombia (2006).
 - ¹⁵ C. P. Patiño Barrera, *Cálculo de las constantes de fuerza entre bases nitrogenadas del ADN. Aplicando el método SIESTA.*, Master's thesis, Universidad Nacional de Colombia (2010).
 - ¹⁶ E. Artancho, J. De la, J. Gale, A. García, J. Junquera, R. M. Martín, P. Ordejón, D. Sánchez, and J. Soler, *USER'S GUIDE SIESTA 3.1* (Fundación General Universidad Autónoma de Madrid, Madrid, 2011).
 - ¹⁷ J. Coraux, A. T. N'Diaye, M. Engler, C. Busse, D. Wall, N. Buckanie, F.-J. M. zu Heringdorf, R. van Gastel, B. Poelsema, and T. Michely, *New J. Phys.* **11**, 023006 (2009).
 - ¹⁸ Y. S. Dedkov, M. Fonin, U. Rüdiger, and C. Laubschat, *Phys. Rev. Lett.* **100**, 107602 (2008).
 - ¹⁹ A. M. B. Goncalves, A. Malachias, M. S. Mazzoni, R. G. Lacerda, and R. Magalhes-Paniago, *Nanotechnology* **23**, 175603 (2012).
 - ²⁰ P. D. Padova, C. Quaresima, C. Ottaviani, P. M. Sheverdyaeva, P. Moras, C. Carbone, D. Topwal, B. Olivieri, A. Kara, H. Oughaddou, B. Aufray, and G. L. Lay, *Appl. Phys. Lett.* **96**, 261905 (2010).
 - ²¹ B. Lalmi, H. Oughaddou, H. Enriquez, A. Kara, S. Vizzini, B. Ealet, and B. Aufray, *Appl. Phys. Lett.* **97**, 223109 (2010).
 - ²² A. Fleurence, R. Friedlein, T. Ozaki, H. Kawai, Y. Wang, and Y. Yamada-Takamura, *Phys. Rev. Lett.* **108**, 245501 (2012).
 - ²³ J. H. Davies, *The physics of low-dimensional semiconductors. An introduction* (Cambridge University Press, 1998).
 - ²⁴ N. Ashcroft and N. Mermin, *Solid State Physics* (Saunders, 1976).
 - ²⁵ A. H. Castro Neto, F. Guinea, N. M. R. Peres, K. S. Novoselov, and A. K. Geim, *Rev. Mod. Phys.* **81**, 109 (2009).
 - ²⁶ K.-C. Chuang, R. S. Deacon, R. J. Nicholas, K. S. Novoselov, and A. K. Geim, *Phil. Trans. R. Soc. A* **366**, 237 (2008).
 - ²⁷ J. Xue, J. Sanchez-Yamagishi, D. Bulmash, P. Jacquod, A. Deshpande, K. Watanabe, T. Taniguchi, P. Jarillo-Herrero, and B. J. LeRoy, *Nat. Mater.* **10**, 282 (2011).
 - ²⁸ H. Şahin, S. Cahangirov, M. Topsakal, E. Bekaroglu, E. Akturk, R. Senger, and S. Ciraci, *Phys. Rev. B* **80**, 155453 (2009).
 - ²⁹ J. C. García, D. B. de Lima, L. V. C. Assali, and J. F. Justo, *J. Phys. Chem. C* **115**, 13242 (2011).
 - ³⁰ M. Houssa, G. Pourtois, V. V. Afanasév, and A. Stesmans, *Appl. Phys. Lett.* **96**, 082111 (2010).
 - ³¹ G. G. Guzmán-Verri and L. C. Lew Yan Voon, *Phys. Rev. B* **76**, 075131 (2007).
 - ³² S. Lebegue and O. Eriksson, *Phys. Rev. B* **79**, 115409 (2009).
 - ³³ T. Suzuki and Y. Yokomizo, *Physica E Low Dimens. Syst. Nanostruct.* **42**, 2820 (2010).
 - ³⁴ A. M. Rojas-Cuervo, C. P. Barrera-Patiño, and R. R. Rey-González, *AIP Conference Proceedings* **1399**, 169 (2011).
 - ³⁵ L. Guohong, L. Adina, and E. Andrei, *Phys. Rev. Lett.* **102**, 176804 (2009).

- ³⁶ D. A. Siegel, C.-H. Park, C. Hwang, J. Deslippe, A. V. Fedorov, S. G. Louie, and A. Lanzara, PNAS **108**, 11365 (2011).
- ³⁷ P. Vogt, P. De Padova, C. Quaresima, J. Avila, E. Frantzeskakis, M. C. Asensio, A. Resta, B. Ealet, and G. Le Lay, Phys. Rev. Lett. **108**, 155501 (2012).
- ³⁸ A. Luican, G. Li, and E. Y. Andrei, Phys. Rev. B **83**, 041405 (2011).
- ³⁹ D. C. Elias, R. V. Gorbachev, A. S. Mayorov, S. V. Morozov, A. A. Zhukov, P. Blake, L. A. Ponomarenko, I. V. Grigorieva, K. S. Novoselov, F. Guinea, and A. K. a. Geim, Nat. Phys. **7**, 701 (2011).
- ⁴⁰ J. González, F. Guinea, and M. Vozmediano, Nucl. Phys. B **424**, 595 (1994).
- ⁴¹ A. M. Rojas-Cuervo and R. R. Rey-González, To be published.